

MASS ESTIMATORS FOR FLATTENED DISPERSION-SUPPORTED GALAXIES

JASON L. SANDERS AND N. WYN EVANS

Institute of Astronomy, Madingley Road, Cambridge, CB3 0HA
 (Dated: Accepted XXX. Received YYY; in original form ZZZ)
Draft version November 5, 2021

ABSTRACT

We investigate the reliability of mass estimators based on the observable velocity dispersion and half-light radius R_h for dispersion-supported galaxies. We show how to extend them to flattened systems and provide simple formulae for the mass within an ellipsoid under the assumption the dark matter density and the stellar density are stratified on the same self-similar ellipsoids. We demonstrate explicitly that the spherical mass estimators (Walker et al. 2009; Wolf et al. 2010) give accurate values for the mass within the half-light ellipsoid, provided R_h is replaced by its ‘circularized’ analogue $R_h\sqrt{1-\epsilon}$. We provide a mathematical justification for this surprisingly simple and effective workaround. It means, for example, that the mass-to-light ratios are valid not just when the light and dark matter are spherically distributed, but also when they are flattened on ellipsoids of the same constant shape.

Keywords: galaxies: dwarf — galaxies: kinematics and dynamics — dark matter

1. INTRODUCTION

Accurate estimates of the dark matter content of dwarf spheroidal galaxies (dSphs) are crucial for furthering our understanding of galaxy formation and structure. Calculating reliable mass estimates has historically been an awkward problem as with only line-of-sight (l.o.s.) velocity measurements the mass profile of a spherical galaxy can only be inferred by making an assumption about the degree of velocity anisotropy i.e. the ratio of radial to tangential motion.

Through comparisons to solutions of the Jeans equations, it has been shown that the mass contained near the half-light radius of a dispersion-supported galaxy is approximately independent of the velocity anisotropy and the radial profile of the dark and luminous matter and is simply related to the half-light radius R_h and the luminosity-averaged l.o.s. velocity dispersion $\sqrt{\langle\sigma_{\text{l.o.s.}}^2\rangle}$. There exist several different forms for these formulae in the literature (Walker et al. 2009; Wolf et al. 2010; Amorisco & Evans 2012; Campbell et al. 2016) that may be summarised as

$$M_{\text{sph}}(< r_x) = \frac{C_x \langle\sigma_{\text{l.o.s.}}^2\rangle R_h}{G} \quad (1)$$

where $M_{\text{sph}}(< r_x)$ is the mass contained within a sphere of radius r_x and G the familiar gravitational constant. C_x is a constant that depends on the choice of radius r_x . Walker et al. (2009) proposed that if $r_x = R_h$ then $C_x = 2.5$ based on a simple example of the stellar distribution following a Plummer profile and the dark matter following a cored isothermal profile although this was validated through fuller testing. Wolf et al. (2010) demonstrated that for $r_x \approx \frac{4}{3}R_h$ (approximately the 3D spherical half-light radius for a range of observationally-motivated profiles) that $C_x = 4$ reproduced the results from full Jeans analyses and was also shown to be mathematically true under the assumption of a near-flat velocity dispersion profile.

Although spherical mass estimators have proved useful for understanding dSphs, they cannot give the full picture as they do not consider the fundamentally aspherical shape of these

galaxies. Our aim in this Letter is to find mass estimators equivalent to equation (1) applicable to flattened systems. We begin by inspecting the validity of the spherical mass estimators and go on to investigate the applicability of the estimator when considering flattened systems in which the dark and light matter are stratified on the same self-similar ellipsoids. We give formulae similar to equation (1) that may be used when the 3D shape of the system is known. By marginalizing over prior assumptions on the intrinsic shape and alignment, we show how the mass can be estimated when the intrinsic shape and alignment are not known.

2. SPHERICAL MASS ESTIMATORS

For a spherical stellar luminosity density $j_*(r)$ with a constant mass-to-light ratio in a spherical mass density $\rho_{\text{DM}}(r)$ with mass profile $M(r)$ sourcing potential $\Phi(r)$, the potential energy can be written in terms of the surface brightness $S(R)$ as

$$W = \frac{1}{2} \int dV j_*(r)\Phi(r) = 4\pi G \int_0^\infty dr I(r)M'(r), \quad (2)$$

where

$$I(r) = \int_r^\infty dr r j_*(r) = -\frac{1}{\pi} \int_r^\infty dR (R^2 - r^2)^{1/2} \frac{dS}{dR} \quad (3)$$

From the virial theorem, we know that the l.o.s. velocity dispersion is related to the total luminosity L by $\langle\sigma_{\text{l.o.s.}}^2\rangle = -W/3L$ which gives the constant C_x as

$$C_x = \frac{1}{R_h} \left[\int_0^{r_x} dr r^2 \rho_{\text{DM}}(r) \right] \left[\int_0^\infty dr r^2 J(r) \rho_{\text{DM}}(r) \right]^{-1} \quad (4)$$

where $J(r) = (4\pi/3L)I(r)$. The constant C_x depends only on the profile of the halo model ρ_{DM} and the surface brightness profile $J(r)$.

We use this to test the validity of the spherical mass estimator. In Fig. 1, we show the result of equation (4) computed numerically for two models with differing ratios of dark to stellar scale-lengths (r_{DM}/R_h). They are an NFW dark matter profile $\rho_{\text{DM}}(r) \propto r^{-1}(1+r/r_{\text{DM}})^{-2}$ and a cored isother-

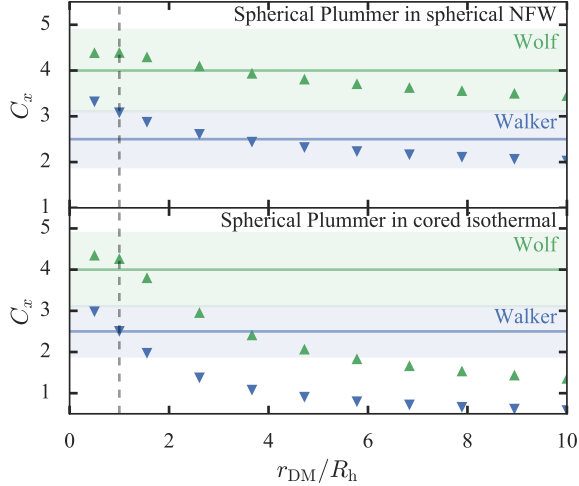


Figure 1. Constant C_x in the spherical mass estimator formula against the ratio of the dark-matter scale radius to the stellar half-light radius for a Plummer model embedded in an NFW (upper panel) and cored isothermal (lower) halo. The blue down-pointing triangles show C_x at the radius $r = R_h$, for which the Walker et al. (2009) advocate a value of $C_x = 2.5$ (shown with a solid blue horizontal line). The green up-pointing triangles show the C_x at the radius $r = \frac{4}{3}R_h$, for which Wolf et al. (2010) advocate a value of $C_x = 4$ (green line). The bands show the uncertainties from Campbell et al. (2016).

mal profile of the form

$$\rho_{\text{DM}}(r) = \frac{v_0^2}{4\pi G} \frac{3r_{\text{DM}}^2 + r^2}{(r_{\text{DM}}^2 + r^2)^2}. \quad (5)$$

The stellar tracer profile follows a Plummer law $\rho_*(r) \propto (1 + (r/r_*)^2)^{-5/2}$ for which $R_h = r_*$. The constant C_x is computed at the two radii recommended by Walker et al. (2009) and Wolf et al. (2010). The constants given by these two authors are shown with horizontal lines along with the uncertainty found by Campbell et al. (2016) from inspecting cosmological hydrodynamical simulations. The variation of C_x with respect to r_{DM}/R_h is smallest for the NFW profile and is consistent with the bracket found by Campbell et al. (2016). In the cored isothermal profile with $r_{\text{DM}}/R_h \approx 1$, both estimators perform well. However, again as r_{DM}/R_h is increased, C_x deviates significantly and so the estimators perform poorly for $r_{\text{DM}}/R_h > 2$.

We now explore how the mass estimators perform as the parameters of a double power-law dark matter density profile are altered. We use a fixed Plummer profile for the stars with a sech truncation at $10R_h$. In Fig. 2, we show the mass profiles of different dark matter profiles that all produce the same luminosity-averaged l.o.s. velocity dispersion. The default parameters are those of an NFW profile with $r_{\text{DM}}/R_h = 1$ and a sech truncation at $10r_{\text{DM}}$. We alter the outer slope β , inner slope γ and the ratio r_{DM}/R_h . We find that when varying the inner and outer slopes the pinch point where the mass is the same for all profiles is around $\frac{4}{3}R_h$ i.e. the radius recommended by Wolf et al. (2010). Varying r_{DM}/R_h produces a pinch point further out. This helps explain why mass estimators derived for use on realistic halos with $r_{\text{DM}} > R_h$ can constrain the mass at larger radii (e.g. Amorisco & Evans 2012; Campbell et al. 2016).

3. FLATTENED MASS ESTIMATORS

We now turn to adapting the spherical mass estimators for application to flattened systems. We work with models with both the dark and stellar density stratified on the same concentric self-similar ellipsoids labelled with the coordinate m such that $m^2 = x^2/a^2 + y^2/b^2 + z^2/c^2$ with $a > b > c$. The axis ratios of the ellipsoids are $p = b/a$ and $q = c/a$. We view the model along the spherical polar unit vector defined by the angles (ϑ, φ) , where ϑ is the co-latitudinal angle and φ the azimuthal angle defined with respect to a Cartesian coordinate system aligned with the principal axes (see Fig. 3). When oblate and prolate spheroids are viewed ‘face-on’, they appear round. The spherical mass estimator underestimates (overestimates) the mass within a sphere for the oblate (prolate) case, as mass is added to (removed from) the sphere. Similarly, the formulae give (smaller) under- and overestimates for the mass within the corresponding ellipsoid. We seek an appropriate modification to equation (1) that is applicable to flattened systems, namely

$$M_{\text{ell}}(< m_x) = \frac{C_x f_\sigma \langle \sigma_{\text{los}}^2 \rangle f_r R_h}{G}, \quad (6)$$

where $M_{\text{ell}}(< m_x)$ is the mass within an ellipsoid (that is the same shape as the equidensity contours) with major axis length r_x . We imagine creating an ellipsoidal model by deforming a spherical model that obeys the spherical mass estimator formulae outlined in the previous section. The total mass is conserved if $abc = 1$ and the mass within an ellipsoid of major-axis length r_x is identical to the mass within a sphere of radius $m_x = r_x/a = r_x(pq)^{1/3}$. However, to estimate this parent spherical model mass from the spherical mass estimator formulae, we must relate the observed l.o.s. velocity dispersion to the spherical velocity dispersion and the observed half-light major-axis length to the intrinsic major-axis length of the considered ellipsoid. Assuming the total velocity dispersion (the average of the dispersions along the principal axes) is conserved as we deform the model¹, the factor f_σ accounts for the relationship between the l.o.s. velocity dispersion and the total dispersion of the ellipsoidal model. The factor f_r accounts for the relationship between the observed major-axis length and the intrinsic major-axis length of the equivalent ellipsoid (and that of the parent spherical model).

3.1. Velocity scaling

For triaxial systems, the velocity scaling $f_\sigma = \langle \sigma_{\text{tot}}^2 \rangle / \langle \sigma_{\text{los}}^2 \rangle$ is given by

$$f_\sigma = \frac{1}{3} \frac{1 + r_{xz} + r_{yz}}{\cos^2 \vartheta + r_{xz} \sin^2 \vartheta \cos^2 \varphi + r_{yz} \sin^2 \vartheta \sin^2 \varphi} \quad (7)$$

where

$$r_{ij} = \langle \sigma_i^2 \rangle / \langle \sigma_j^2 \rangle = W_{ii} / W_{jj} \text{ (no sum)}. \quad (8)$$

For dSphs in which the stellar and dark-matter density profiles are stratified on the same self-similar ellipsoids, r_{ij} depends only on the shape of the ellipsoids (Roberts 1962; Binney & Tremaine 2008). That is to say, it is independent of the ‘radial’ density profile of the light and dark matter.

¹ To leading order in the flattening, the ratio of the total dispersion of the flattened model to the spherical model with the same mass is $\langle \sigma_{\text{tot}}^2 \rangle_{\text{flat}} / \langle \sigma_{\text{tot}}^2 \rangle_{\text{sph}} \approx 1 - \frac{4}{45} [(1-p)^2 - (1-p)(1-q) + (1-q)^2]$.

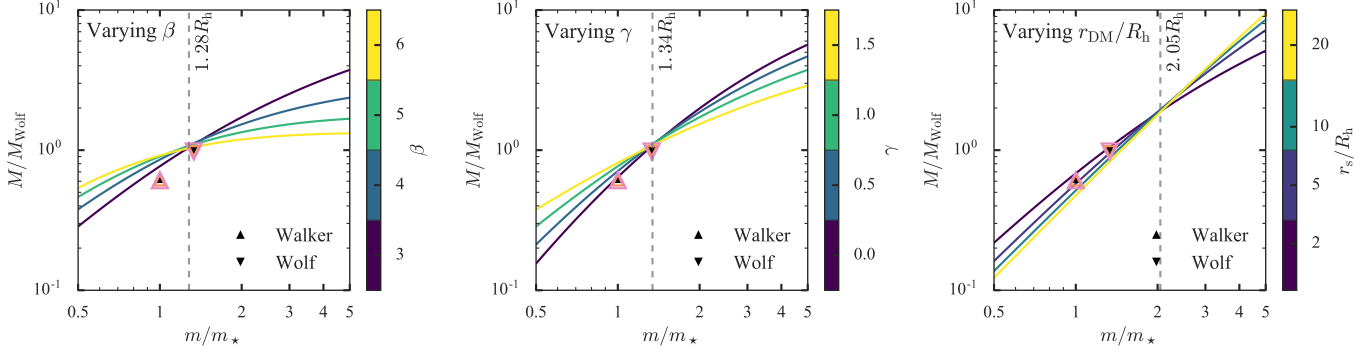


Figure 2. Spheroidal mass profile for a stellar Plummer profile embedded in a double power-law dark-matter halo with varying outer slope β , inner-slope γ and scale radius r_{DM} . All models have the same luminosity-averaged I.o.s. velocity dispersion and half-light radius R_h . The masses are normalized with respect to the Wolf mass estimate. The default parameters are $\gamma = 1$, $\beta = 3$ (NFW) and $r_s/R_h = 1$. The black points show the results of two mass estimators and the vertical dashed line shows the point of minimum variance in the logarithm of the mass for each set of curves. The spheroidal mass estimates using the mass estimator proposed in this paper are given for an edge-on oblate ($q = 0.6$, orange triangles) and edge-on prolate model ($p = q = 0.6$, pink triangles).

Therefore, f_σ is a function of p , q and the viewing angles: $f_\sigma = f_\sigma(\vartheta, \varphi, p, q)$. Expressions for W_{ij} are given in Table 2.2 of Binney & Tremaine (2008).

3.2. Radial scaling

We decompose the radial scaling into two components, $f_r = f_1 f_2$. f_2 describes the relationship between the ellipsoidal major-axis length and the parent spherical radius so (as described above) $f_2 = (pq)^{1/3}$. The other factor f_1 gives the relationship between the observed major-axis length of the half-light ellipse R_h and the intrinsic major-axis length of the corresponding ellipsoid r_{maj} . In the spherical case, these quantities are equal. In the ellipsoidal case, the relationship between these quantities depends on the viewing angles and the intrinsic shape $f_1 = f_1(\vartheta, \varphi, p, q)$. We approximate f_1 by the relationship between the major-axis length of an ellipsoid and the major-axis length of its projected ellipse. This neglects any subtleties related to the extended nature of the true density distribution. However, if the 3D stellar light profile falls off sufficiently rapidly then our relationship is a good approximation.

To derive our approximation for f_1 , we use a coordinate system (x', y', z') related to the intrinsic coordinate system by (see Fig. 3)

$$\begin{aligned} x &= -x' \sin \varphi - y' \cos \vartheta \cos \varphi + z' \sin \vartheta \cos \varphi \\ y &= x' \cos \varphi - y' \cos \vartheta \sin \varphi + z' \sin \vartheta \sin \varphi \\ z &= y' \sin \vartheta + z' \cos \vartheta. \end{aligned} \quad (9)$$

We consider the set of points where the ellipsoidal surface is tangential to \hat{z}' which results in a rotated ellipse in the (x', y') plane. We diagonalize the resultant quadratic surface to find the major axis length R_h as

$$f_1^{-2} = (R_h/r_{\text{maj}})^2 = 2C/(A - \sqrt{B}), \quad (10)$$

where

$$\begin{aligned} A &= (1 - q^2) \cos^2 \vartheta + (1 - p^2) \sin^2 \vartheta \sin^2 \varphi + p^2 + q^2, \\ B &= [(1 - q^2) \cos^2 \vartheta - (1 - p^2) \sin^2 \vartheta \sin^2 \varphi - p^2 + q^2]^2 \\ &\quad + 4(1 - p^2)(1 - q^2) \sin^2 \vartheta \cos^2 \vartheta \sin^2 \varphi, \\ C &= p^2 \cos^2 \vartheta + q^2 \sin^2 \vartheta (p^2 \cos^2 \varphi + \sin^2 \varphi). \end{aligned} \quad (11)$$

As given in Weijmans et al. (2014), the observed ellipticity ϵ satisfies $(1 - \epsilon)^2 = (A - \sqrt{B})/(A + \sqrt{B})$.

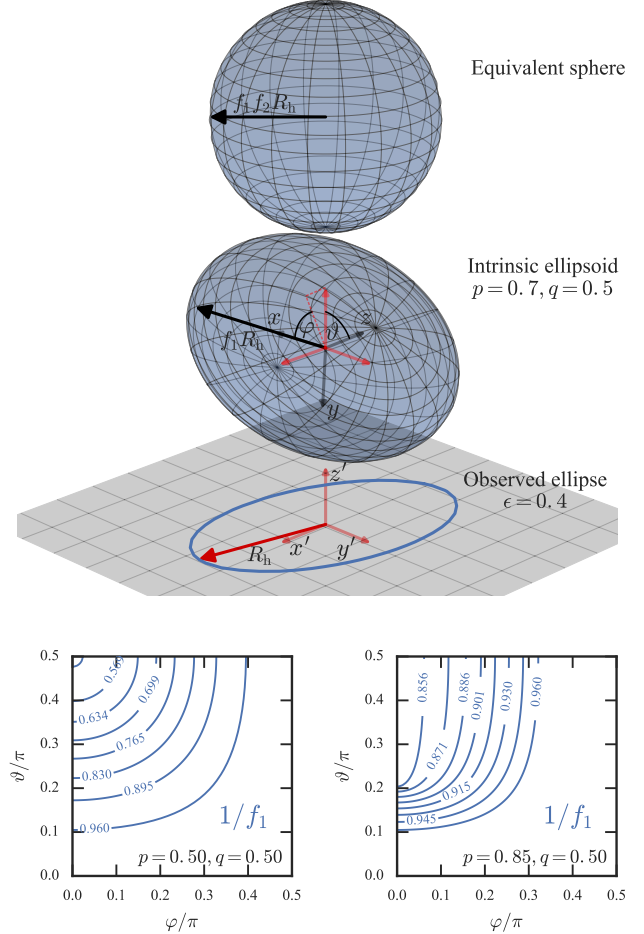


Figure 3. Relationship between the observed half-light radius and the radius used in our mass estimator formula. An ellipsoid is observed at spherical polar angles (ϑ, φ) with respect to its intrinsic Cartesian coordinates (x, y, z) aligned with the principal axes. The resulting projection is an ellipse (shown below) with major-axis length R_h which lies in the (x', y') plane of the observed Cartesian coordinate system (x', y', z') . Above the ellipsoid, we show the sphere with the equivalent volume as the ellipsoid. The major-axis of the ellipse is related to the major-axis of the ellipsoid by the factor $1/f_1$ which is shown in the lower two panels for a prolate spheroid with $p = q = 0.5$ (left) and an ellipsoid with axis ratios $p = 0.85$ and $q = 0.5$ (right).

For an oblate spheroid ($p = 1$), eqn (10) simplifies to $R_h = r_{\text{maj}}$. For a prolate spheroid $p = q$, so we find

$$f_1^{-2} = \cos^2 \vartheta + \sin^2 \vartheta (q^2 \cos^2 \varphi + \sin^2 \varphi). \quad (12)$$

In Fig 3, we show the major axis length for a prolate figure and a triaxial figure as a function of the viewing angle.

The ellipsoidal half-light radius m_h is well approximated by $\frac{4}{3}f_r R_h$ which should be compared to the radius of $\frac{4}{3}R_h \sqrt{1 - \epsilon}$ that is empirically used (e.g. [Koposov et al. 2015](#); [Sanders et al. 2016](#)) as $R_h \sqrt{1 - \epsilon}$ approximately reproduces the circularly-averaged half-light radius of the dSph².

3.3. Near-spherical limits

Using eqn (10), we can find the modification factor $f_\sigma f_r$ for the simple cases of viewing down the principal axes of a near-spherical triaxial ellipsoid and compare to the alternative factor $\sqrt{1 - \epsilon}$. When viewing down the major axis ($\vartheta = \pi/2, \varphi = 0$), we find

$$f_\sigma f_r \approx 1 + \frac{2}{5}(1 - p) - \frac{3}{5}(1 - q). \quad (13)$$

The observed ellipticity $\epsilon = 1 - p/q$ so the *circularized* factor $\sqrt{1 - \epsilon} \approx 1 + \frac{1}{2}(1 - p) - \frac{1}{2}(1 - q)$ which is a close approximation to our factor $f_\sigma f_r$. Similarly, for viewing down the intermediate axis, we find

$$f_\sigma f_r \approx 1 + \frac{1}{5}(1 - p) - \frac{3}{5}(1 - q), \quad (14)$$

whilst $\sqrt{1 - \epsilon} = \sqrt{q} \approx 1 - \frac{1}{2}(1 - q)$. Finally, viewing down the minor axis, we find

$$f_\sigma f_r \approx 1 - \frac{3}{5}(1 - p) + \frac{1}{5}(1 - q), \quad (15)$$

whilst $\sqrt{1 - \epsilon} = \sqrt{p} \approx 1 - \frac{1}{2}(1 - p)$. We note that the flattening in the line-of-sight direction (e.g. p in the intermediate axis case) has a smaller contribution to the factor $f_\sigma f_r$. This demonstrates that the simple factor $\sqrt{1 - \epsilon}$ goes a long way to account for the velocity and radial scalings we propose.

3.4. Results

In Fig. 2, we show the mass estimates using our formulae for an oblate and prolate model viewed edge-on. The models have the same ellipsoidal mass profile as the spherical model shown. The factors we have introduced correctly deproject the observed quantities producing an unbiased mass estimate. Fig. 4 shows the constant in the half-light ellipsoid mass estimator (eqn. (6)) for three models of flattened Plummer profiles embedded in equivalently flattened NFW halos with $m_{\text{DM}}/m_\star = 5$. We show an oblate, prolate and triaxial $p = \frac{1}{2}(1 + q)$ model. Simply using the spherical mass estimator with R_h underestimates/overestimates the ellipsoidal mass for the oblate/prolate case viewed face-on (down the minor/major axis). Similarly, the edge-on case (major for oblate, minor for prolate) produces overestimates of the mass for both oblate and prolate models. For the triaxial model the spherical mass estimator produces an overestimate when viewing down the major axis and (for this particular case) is largely unbiased when viewing down the minor axis. The results using the correction factors f_σ and f_r are unbiased estimates of

² For example, a flattened ($q = 1 - \epsilon$) Plummer surface profile produces a circularly-averaged half-light radius equal to $R_h \sqrt{\frac{1}{6}(1 + q^2 + \sqrt{1 + 14q^2 + q^4})}$ which for small flattenings is $R_h(1 - \frac{1}{2}\epsilon + \mathcal{O}(\epsilon^4))$ so well approximated by $R_h \sqrt{1 - \epsilon}$.

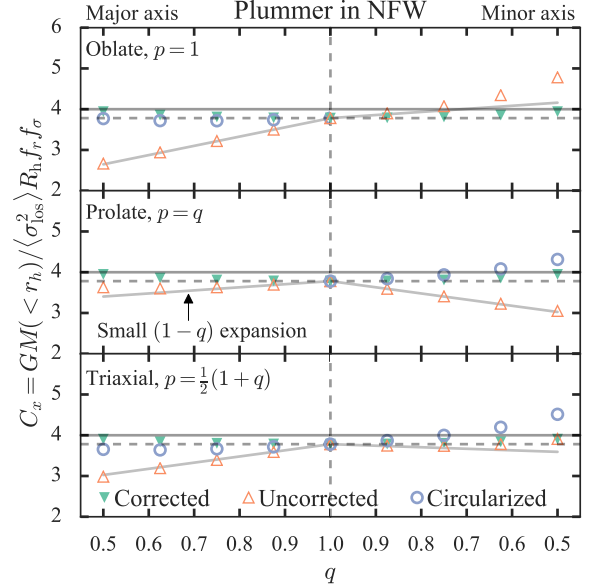


Figure 4. Mass estimator constant for the half-light ellipsoid against the flattening q for Plummer models embedded in equivalently flattened NFW halos. The top panel shows an oblate model, the middle panel a prolate model and the bottom panel a triaxial model with $p = \frac{1}{2}(1 + q)$. The left half of the plot corresponds to viewing down the major axis whilst the right half corresponds to viewing down the minor axis. The *corrected* green filled triangles show the constant from the mass estimator formula given in this paper, the *uncorrected* orange empty triangles show the constant using the spherical mass estimator (i.e. $f_r f_\sigma = 1$) and the purple circles show the constant using the spherical mass estimator with the *circularized* radius $R_h \sqrt{1 - \epsilon}$ (not shown in the panels where $\epsilon = 0$). The horizontal solid line shows the [Wolf et al.](#) constant and the dashed line shows the constant from the spherical model for this exact case. The other gray solid lines show the small $(1 - q)$ expansion of $C_x f_\sigma f_r$ (i.e. the uncorrected constant).

the mass within the ellipsoid $m = \frac{4}{3}m_\star$ and using the spherical mass estimator with the ‘circularized’ radius $R_h \sqrt{1 - \epsilon}$ produces very similar results to the corrected version. This echoes a result in [Sanders et al. \(2016\)](#) who demonstrated that the correction to the D-factor (important for interpreting dark-matter decay signals) is almost independent of the flattening for edge-on systems. The near-spherical expansions of § 3.3 are also shown, which replicate the trends over the full q range.

Our proposed modifications correctly reproduce the mass within ellipsoids. However, this relies on knowing the intrinsic shape and alignment of the dSph. Such information is not accessible, but we can put priors on possible models which reproduce the observables. We choose to put priors on the triaxiality $T = (1 - p^2)/(1 - q^2)$, flattening q and the viewing angles (ϑ, φ). We consider three priors:

1. Flat prior – $T \sim \mathcal{U}(0, 1)$, $q \sim \mathcal{U}(0.05, 1)$, $\cos \vartheta \sim \mathcal{U}(0, 1)$, $\varphi \sim \mathcal{U}(0, \pi/2)$.
2. Major-axis prior – $T \sim \mathcal{U}(0, 1)$, $q \sim \mathcal{U}(0.05, 1)$, $\vartheta \sim \mathcal{N}(\pi/2, 0.1 \text{ rad})$, $\varphi \sim \mathcal{U}(0, 0.1 \text{ rad})$.
3. Fixed-shape prior – $T \sim \mathcal{N}(0.55, 0.04)$, $q \sim \mathcal{N}(0.49, 0.12)$, $\cos \vartheta \sim \mathcal{U}(0, 1)$, $\varphi \sim \mathcal{U}(0, \pi/2)$.

where the final prior is taken from a fit to the shapes of the Local Group dSphs from [Sánchez-Janssen et al. \(2016\)](#). The major-axis prior is inspired by the observation from simulations that the major-axes of subhaloes points towards the cen-

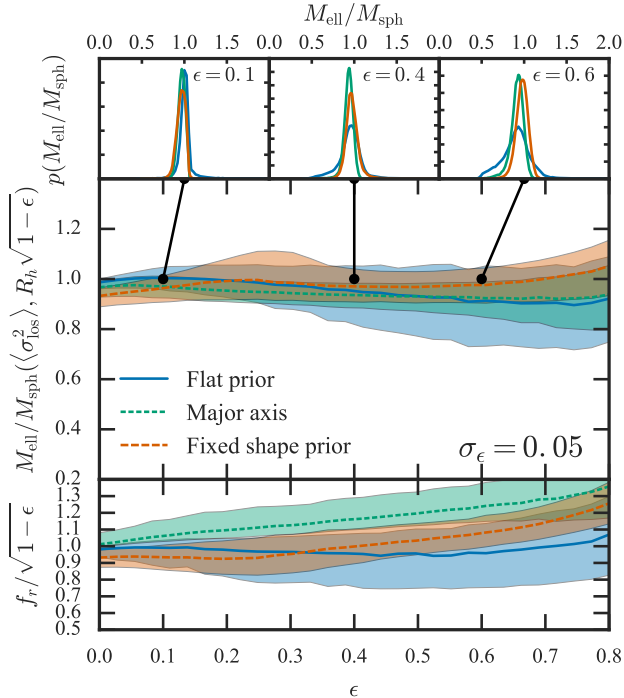


Figure 5. Ratio of the mass within the half-light ellipsoid to the mass estimated from the spherical mass estimator (Walker et al. 2009; Wolf et al. 2010) using the *circularized* half-light radius $R_h\sqrt{1-\epsilon}$ against ellipticity. At each ellipticity we show the median and $\pm 1\sigma$ spreads in the mass estimates for triaxial figures within a 0.05 spread of the required ellipticity and with fixed R_h and $\langle\sigma_{\text{los}}^2\rangle^{1/2}$ under three prior assumptions: the blue solid line corresponds to a uniform prior on viewing angle, intrinsic ellipticity and triaxiality, the green short-dashed line corresponds to a prior of preferentially viewing down the major-axis and the orange long-dashed line corresponds to a fixed triaxiality and intrinsic ellipticity prior. The three histograms show slices through the main figure at $\epsilon = 0.1, 0.4$ and 0.6 . The lower panel shows the median and $\pm 1\sigma$ brackets of $f_r/\sqrt{1-\epsilon}$ – the ratio of the dSph radius to the ‘circularized’ radius.

tre of the host halo (e.g. Barber et al. 2015). We sample from the priors folded with a normal distribution on the observed ellipticity with width $\sigma_\epsilon = 0.05$ (using *emcee* Foreman-Mackey et al. 2013) and for each sample compute the mass within the half-light ellipsoid from equation (6). The results for a range of observed ellipticities are shown in Fig. 5. We show the mass estimates over the spherical mass estimator using the ‘circularized’ radius. We see that using the spherical mass estimator in this way reproduces the mass within the half-light ellipsoid over the full range of ellipticities³. The uncertainty in the estimator increases with increasing ellipticity but is only $\sim 10 - 20$ per cent for $\epsilon \sim 0.4$ (a typical dSph flattening). There is the tendency for the mass within the half-light ellipsoid to be overestimated for large ϵ , but only by ~ 5 per cent. We also show the distribution of $f_r/\sqrt{1-\epsilon}$ for each prior assumption (i.e. the ratio of the size of the ellipsoid to the $R_h\sqrt{1-\epsilon}$ approximation). For the uniform prior, this ratio is unity (within $\sim 10 - 20$ per cent) so the ‘size’ of the dSphs are well approximated by $R_h\sqrt{1-\epsilon}$. For the other two priors, the ratio increases with ellipticity as the intrinsic ellipsoids are on average more elongated along the line-of-sight so

³ We note that a similar observation was made by Laporte et al. (2013) who found that the variations of R_h and $\langle\sigma_{\text{los}}^2\rangle$ with triaxiality compensated each other to give an unbiased mass estimate.

larger than $R_h\sqrt{1-\epsilon}$.

We have demonstrated that the mass within the half-light ellipsoid can be accurately estimated using the spherical mass estimator formulae. Although we do not know the shape or orientation of this half-light ellipsoid, we can say with confidence the mass within it. Therefore, we can accurately estimate the mass-to-light ratio using the mass within the half-light ellipsoid and half the total luminosity L . We conclude that using the spherical mass estimators (Walker et al. 2009; Wolf et al. 2010) with the ‘circularized’ half-light radius produces accurate estimates of the mass-to-light ratio of dSphs, irrespective of flattening, provided the light and dark matter are stratified on the same self-similar concentric ellipsoids.

4. CONCLUSIONS

This Letter has answered the question: how should the mass of a flattened, dispersion-supported galaxy like a dwarf spheroidal be estimated? If the galaxy were spherical, then the answer is well-established. Accurate mass estimators depending on the observable half-light radius and the velocity dispersion of the stars have been devised by a number of investigators (Walker et al. 2009; Wolf et al. 2010; Amorisco & Evans 2012; Campbell et al. 2016).

We have shown how to modify the spherical mass estimators so that they work for flattened systems in which the light and dark matter are stratified on the same concentric self-similar ellipsoids. This represents a limiting case as simulations indicate the dark matter distribution is in fact rounder than the light (Abadi et al. 2010; Zemp et al. 2012) due to baryonic feedback effects, particularly for the more massive dSphs. The modifications require knowledge of the intrinsic shape and alignment of the triaxial figure and reproduce the mass within ellipsoids by deprojecting the half-light radius and line-of-sight velocity dispersion. The resulting mass estimates are independent of details of the radial profile and are as accurate as the corresponding spherical formulae.

This would be of little use if we require knowledge of intrinsic properties. However, we have also shown that, when averaging over triaxial configurations that are consistent with the observed ellipticity ϵ , major-axis half-light length R_h and line-of-sight velocity dispersion, the mass within the half-light ellipsoid is well approximated by the spherical mass estimate using the ‘circularized’ half-light radius of $R_h\sqrt{1-\epsilon}$. The scatter in the estimate increases with ellipticity but is only $10 - 20$ per cent for $\epsilon \sim 0.6$. In turn, this observation implies that mass-to-light ratios using spherical estimators, together with a luminosity of $L_{1/2} = L/2$, are accurate and insensitive to the flattening of the dSph. This therefore provides a surprisingly simple, flexible and effective way to account for the effects of flattening.

REFERENCES

- Abadi, M. G., Navarro, J. F., Fardal, M., Babul, A., & Steinmetz, M. 2010, *MNRAS*, 407, 435
- Amorisco, N. C., & Evans, N. W. 2012, *MNRAS*, 419, 184
- Barber, C., Starkenburg, E., Navarro, J. F., & McConnachie, A. W. 2015, *MNRAS*, 447, 1112
- Binney, J., & Tremaine, S. 2008, *Galactic Dynamics: Second Edition* (Princeton University Press)
- Campbell, D. J. R., Frenk, C. S., Jenkins, A., et al. 2016, *ArXiv e-prints*, arXiv:1603.04443
- Foreman-Mackey, D., Conley, A., Meierjürgen Farr, W., et al. 2013, emcee: The MCMC Hammer, , *astrophysics Source Code Library*, ascl:1303.002
- Koposov, S. E., Belokurov, V., Torrealba, G., & Evans, N. W. 2015, *ApJ*, 805, 130
- Laporte, C. F. P., Walker, M. G., & Peñarrubia, J. 2013, *MNRAS*, 433, L54
- Roberts, P. H. 1962, *ApJ*, 136, 1108
- Sánchez-Janssen, R., Ferrarese, L., MacArthur, L. A., et al. 2016, *ApJ*, 820, 69
- Sanders, J. L., Evans, N. W., Geringer-Sameth, A., & Dehnen, W. 2016, *ArXiv e-prints*, arXiv:1604.05493
- Walker, M. G., Mateo, M., Olszewski, E. W., et al. 2009, *ApJ*, 704, 1274
- Weijmans, A.-M., de Zeeuw, P. T., Emsellem, E., et al. 2014, *MNRAS*, 444, 3340
- Wolf, J., Martinez, G. D., Bullock, J. S., et al. 2010, *MNRAS*, 406, 1220
- Zemp, M., Gnedin, O. Y., Gnedin, N. Y., & Kravtsov, A. V. 2012, *ApJ*, 748, 54